Causes and Implications of Persistent Atmospheric Carbon Dioxide Biases in Earth System Models

Forrest M. Hoffman[1,2], James T. Randerson[1], Vivek K. Arora[3], Qing Bao[4], Katharina D. Six[5], Patricia Cadule[6], Duoying Ji[7], Chris D. Jones[8], Michio Kawamiya[9], Samar Khatiwala[10], Keith Lindsay[11], Atsushi Obata[12], Elena Shevliakova[13], Jerry F. Tjiputra[14], Evgeny M. Volodin[15], Tongwen Wu[16]

[1]Department of Earth System Sciences, University of California, Irvine, California 92697, USA; [2]Computational Earth Sciences Group, Oak Ridge National Laboratory, Oak Ridge, Tennessee 37831, USA; [3]Canadian Centre for Climate Modelling and Analysis, Meteorological Service of Canada, Victoria, BC, V8W 3V6, Canada; [4]State Key Laboratory of Numerical Modeling for Atmospheric Sciences and Geophysical Fluid Dynamics, Institute of Atmospheric Physics, Chinese Academy of Sciences, Beijing 100029, China; [5]Max Planck Institute for Meteorology, Bundesstraße 53, 20146 Hamburg, Germany; [6]Institut Pierre Simon Laplace, Laboratoire des Sciences du Climat et de l'Environnement, 91191 Gif sur Yvette Cedex, France; [7]State Key Laboratory of Earth Surface Processes and Resource Ecology, College of Global Change and Earth System Science, Beijing Normal University, Beijing 100875, China; [8]Hadley Centre, U.K. Met Office, Exeter, EX1 3PB, United Kingdom; [9]Research Institute for Global Change, Japan Agency for Marine-Earth Science and Technology, Yokosuka-city, Kanagawa, Japan; [10]Lamont Doherty Earth Observatory, Columbia University, Palisades, New York 10964, USA; [11]Climate & Global Dynamics Division, National Center for Atmospheric Research, Boulder, Colorado 80307, USA; [12]Meteorological Research Institute, Japan Meteorological Agency, Tsukuba-city, Ibaraki, Japan; [13]Geophysical Fluid Dynamics Laboratory, Princeton University, Princeton, New Jersey 08540, USA; [14]Uni Climate, Uni Research, Allégaten 70, 5007 Bergen, Norway; [15]Institute of Numerical Mathematics, Russian Academy of Science, Moscow, 119333, Russia; [16]Climate System Modeling Division, Beijing Climate Center, China Meteorological Administration, Beijing 100081, China.

Abstract

The strength of feedbacks between a changing climate and future CO_2 concentrations are uncertain and difficult to predict using Earth System Models (ESMs). We analyzed emissions-driven simulations—in which atmospheric CO_2 levels were computed prognostically—for historical (1850–2005) and future periods (RCP 8.5 for 2006–2100) produced by 15 ESMs for the Fifth Phase of the Coupled Model Intercomparison Project (CMIP5). Comparison of ESM prognostic atmospheric CO_2 over the historical period with observations indicated that ESMs, on average, had a small positive bias in predictions of contemporary atmospheric CO_2. A key driver of this persistent bias was weak ocean carbon uptake exhibited by the majority of ESMs, based on comparisons with observations of ocean and atmosphere anthropogenic carbon inventories. We exploited a significant linear relationship found between the magnitude of contemporary and future atmospheric CO_2 levels to create a contemporary CO_2 tuned model (CCTM) estimate of the trajectory for the 21st century. The CCTM yielded CO_2 estimates of 600 ± 14 ppm at 2600 and 947 ± 35 ppm at 2100, which were 21 ppm and 32 ppm below the multi-model mean during these two time periods. Uncertainty estimates derived from this approach were almost 6 times smaller at 2060 and almost 5 times smaller at 2100 than those from the ESM ensemble. The CCTM also significantly narrowed the range of CO_2-induced radiative forcing and temperature increases during the remainder of the 21st century. Because many processes contributing to contemporary carbon cycle biases persist over decadal timescales, our analysis suggests uncertainties in future climate scenarios may be considerably reduced by tuning models to the long-term time series of CO_2 from Mauna Loa and other atmospheric monitoring stations.

Description of Models

Table 1: *Models that generated output used in this study.*

Model	Modeling Center (or Group)	Component Models and Resolutions: Atmosphere	Land	Ocean	Sea Ice
BCC-CSM1.1 (Wu et al., 2013)	Beijing Climate Center, China Meteorological Administration, CHINA	AGCM2.1 ($2.875^\circ \times 2.875^\circ$, L26)	BCC_AVIM1.0 ($2.875^\circ \times 2.875^\circ$)	MOM4_L40 ($1^\circ \times (1–\frac{1}{3})^\circ$, L40)	SIS ($1^\circ \times (1–\frac{1}{3})^\circ$)
BCC-CSM1.1(m) (Wu et al., 2013)	Beijing Climate Center, China Meteorological Administration, CHINA	AGCM2.2 ($1.125^\circ \times 1.125^\circ$, L26)	BCC_AVIM1.0 ($1.125^\circ \times 1.125^\circ$)	MOM4_L40 ($1^\circ \times (1–\frac{1}{3})^\circ$, L40)	SIS ($1^\circ \times (1–\frac{1}{3})^\circ$)
BNU-ESM†f (Dai et al., 2003, 2004; College of Global Change and Earth System Science, 2012)	Beijing Normal University, CHINA	CAM3.5 ($2.875^\circ \times 2.875^\circ$, L26)	CoLM3 & BNUDGVM (C/N) ($2.875^\circ \times 2.875^\circ$, L10)	MOM4p1 & IBGC ($1^\circ \times (1–\frac{1}{3})^\circ$, L50)	CICE4.1 ($1^\circ \times (1–\frac{1}{3})^\circ$)
CanESM2‡ (Arora et al., 2011)	Canadian Centre for Climate Modelling and Analysis, CANADA	CanAM4 ($2.81^\circ \times 2.81^\circ$, L35)	CLASS2.7 & CTEM1 ($2.81^\circ \times 2.81^\circ$)	CanOM4 & CMOC1.2 ($1.5^\circ \times 1^\circ$, L40)	CanSIM1 ($2.81^\circ \times 2.81^\circ$)
CESM1-BGCf (Hurrell et al., in press; Keppel-Aleks et al., in press; Lindsay et al., in review)	Community Earth System Model Contributors, NSF-DOE-NCAR, USA	CAM4 ($0.9^\circ \times 1.25^\circ$, L30)	CLM4 ($0.9^\circ \times 1.25^\circ$)	POP2 & NPZD ($1^\circ \times (1–\frac{1}{3})^\circ$, L60)	CICE4 ($1^\circ \times (1–\frac{1}{3})^\circ$)
FGOALS-s2.0a (Bao et al., in press; Liu et al., 2012; Lin et al., 2013)	LASG, Institute of Atmospheric Physics, CAS, CHINA	SAMIL2.4.7 ($1.67^\circ \times 2.81^\circ$, L26)	CLM3 & VEGAS2.0 ($1.67^\circ \times 2.81^\circ$)	LICOM2.0 ($1^\circ \times (1–\frac{1}{2})^\circ$, L30)	CSIM5 ($1^\circ \times (1–\frac{1}{2})^\circ$)
GFDL-ESM2g, GFDL-ESM2mb (Dunne et al., 2012, 2013)	NOAA Geophysical Fluid Dynamics Laboratory, USA	AM2 ($2^\circ \times 2.5^\circ$, L24)	LM3 ($2^\circ \times 2.5^\circ$)	MOM4 ($1^\circ \times (1–\frac{1}{3})^\circ$, L50)	SIS ($1^\circ \times (1–\frac{1}{3})^\circ$)
HadGEM2-ESc (Collins et al., 2011; Jones et al., 2011)	Met Office Hadley Centre, UNITED KINGDOM	HadGAM2 & UKCA ($1.25^\circ \times 1.875^\circ$, L38)	MOSES2 & TRIFFID ($1.25^\circ \times 1.875^\circ$)	HadGOM2 & diat-HadOCC ($1^\circ \times (1–\frac{1}{3})^\circ$, L40)	HadGOM2 ($1^\circ \times (1–\frac{1}{3})^\circ$)
INM-CM4†‡ (Volodin et al., 2010)	Institute for Numerical Mathematics, RUSSIA	($2^\circ \times 1.5^\circ$, L21)	($2^\circ \times 1.5^\circ$)	($1^\circ \times 0.5^\circ$, L40)	($1^\circ \times 0.5^\circ$)
IPSL-CM5A-LRd (Dufresne et al., 2013)	Institut Pierre-Simon Laplace, FRANCE	LMDZ4 ($3.75^\circ \times 1.9^\circ$, L39)	ORCHIDEE ($3.75^\circ \times 1.9^\circ$)	ORCA2 & PISCES ($2^\circ \times (2–\frac{1}{2})^\circ$, L31)	LIM2 ($2^\circ \times (2–\frac{1}{2})^\circ$)
MIROC-ESMf (Watanabe et al., 2011; Oschlies, 2001)	Japan Agency for Marine-Earth Science and Technology, Atmosphere and Ocean Research Institute (University of Tokyo), and National Institute for Environmental Studies, JAPAN	MIROC-AGCM & SPRINTARS ($2.875^\circ \times 2.875^\circ$, L80)	MATSIRO & SEIB-DGVM ($2.875^\circ \times 2.875^\circ$, L6)	COCO3.4 & NPZD ($1.5^\circ \times 1^\circ$, L44)	COCO3.4 ($1.5^\circ \times 1^\circ$)
MPI-ESM-LRef (Maier-Reimer et al., 2005; Raddatz et al., 2007; Brovkin et al., 2009)	Max Planck Institute for Meteorology, GERMANY	ECHAM6 ($2.81^\circ \times 2.81^\circ$, L47)	JSBACH ($2.81^\circ \times 2.81^\circ$)	MPIOM & HAMOCC ($1.5^\circ \times 1.5^\circ$, L40)	MPIOM ($1.5^\circ \times 1.5^\circ$)
MRI-ESM1 (Yukimoto et al., 2011; Nakano et al., 2011; Yukimoto et al., 2012; Obata and Shibata, 2012)	Meteorological Research Institute, JAPAN	GSMUV ($0.75^\circ \times 0.75^\circ$, L48)	HAL & MRI-LCCM2 ($0.75^\circ \times 0.75^\circ$)	MRI.COM3 ($1^\circ \times 0.5^\circ$, L51)	MRI.COM3 ($1^\circ \times 0.5^\circ$)
NorESM1-ME (Bentsen et al., 2012; Iversen et al., 2013; Tjiputra et al., 2013)	Norwegian Climate Centre, NORWAY	CAM4-Oslo ($1.9^\circ \times 2.5^\circ$, L26)	CLM4 ($1.9^\circ \times 2.5^\circ$)	MICOM & HAMOCC ($1^\circ \times (1–\frac{1}{3})^\circ$, L53)	CICE4 ($1^\circ \times (1–\frac{1}{3})^\circ$)

†Atmospheric CO_2 required unit correction.
‡Ocean carbon flux required unit correction.
aFGOALS-s2 model provided no ocean carbon fluxes.
bGFDL-ESM2g and GFDL-ESM2m output available beginning January 1861.
cHadGEM2-ES output available for December 1859 through November 2099; annual atmospheric CO_2 obtained directly from Hadley Centre.
dIPSL-CM5A-LR monthly atmospheric CO_2 obtained directly from IPSL.
eMPI-ESM-LR provided three *esmHistorical* realizations and one *esmrcp85* realization.
fAtmospheric CO_2 mole fraction was computed from 3-dimensional output.

Observations and Calculations

- We used an observationally based estimate of anthropogenic CO_2 uptake by the ocean, produced by Khatiwala et al. (2009, 2012) using a Green's function model for ocean tracer transport, in combination with observed atmospheric CO_2 and fossil fuel emission estimates to assess model biases in carbon accumulation in the atmosphere, ocean, and land reservoirs.
- We adopted a strategy similar to that of Hall and Qu (2006) to constrain future trends in atmospheric CO_2 using contemporary observations to create the CCTM.
- We employed an impulse response function to estimate temperature changes based on time-integrated changes in radiative forcing to evaluate the implications of model CO_2 biases.

Contemporary Biases in Atmospheric CO_2

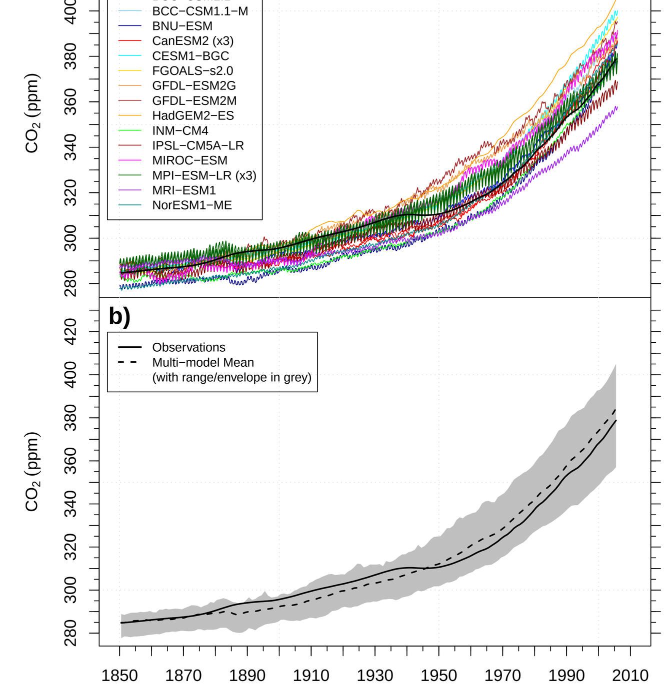

Figure 1: *(a) Most ESMs exhibit a high bias in atmospheric CO_2 mole fraction. The predicted atmospheric CO_2 mole fraction for the 19 historical simulations shown here ranges from 357–405 ppm at the end of the CMIP5 historical period (1850–2005). (b) The multi-model mean is biased high from 1946 throughout the 20th century, ending 5.6 ppm above observations in 2005.*

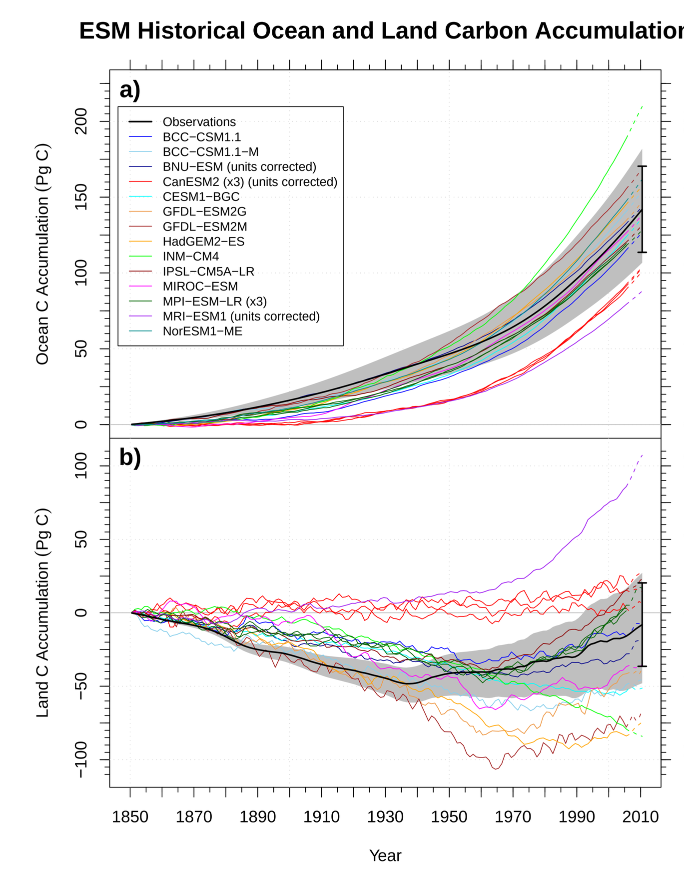

Figure 2: *(a) Ocean and (b) land anthropogenic carbon inventories from CMIP5 models compared to estimates from Khatiwala et al. (2012). Most ESMs exhibit a low bias in ocean anthropogenic carbon accumulation from 1870–1930 as compared with adjusted estimates from Khatiwala et al. (2012). ESMs had a wide range of land carbon accumulation responses to increasing atmospheric CO_2 and land use change, ranging from a cumulative source of 84 Pg C to a cumulative sink of 107 Pg C in 2010.*

Causes and Implications of the Contemporary Bias

- A key driver of the persistent high bias was weak ocean carbon uptake exhibited by the majority of ESMs.
- The high atmospheric CO_2 bias for the multi-model mean produced radiative forcing that was too large and, consequently, an unrealistically high temperature increase during the historical period.
- We will see that the atmospheric CO_2 bias persists into the future, causing large and divergent model projections during the 21st century.

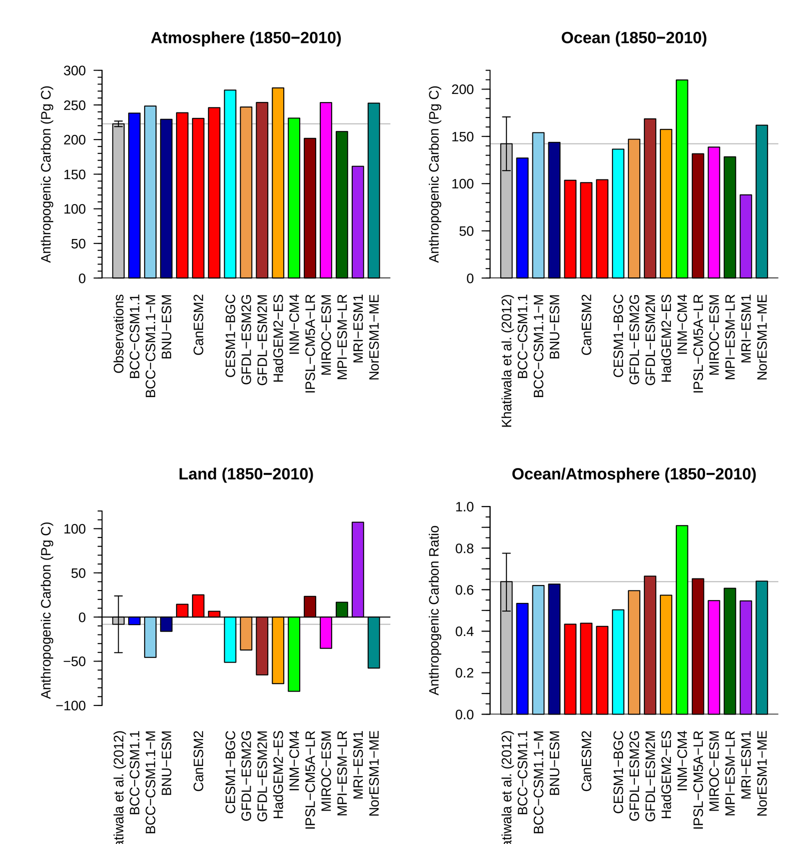

Figure 3: *Reconstructed atmospheric CO_2 levels and observationally based estimates of ocean carbon uptake from Khatiwala et al. (2012) provide constraints on carbon inventories in the ocean, and on land when combined with fossil fuel and atmospheric CO_2 observations. While ocean carbon accumulation appears adequate in some model results, ocean carbon accumulation in most ESMs show a low bias once normalized by atmospheric accumulation (lower right panel).*

Persistence of Biases into the Future

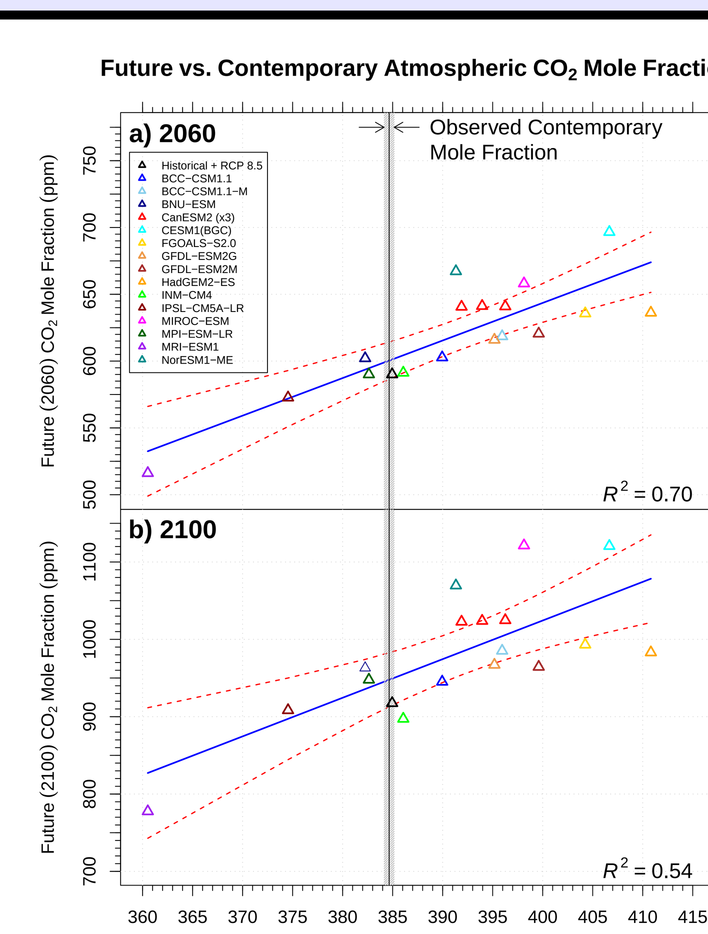

Figure 4: *(a) Future (2060) vs. contemporary (2010) atmospheric CO_2 mole fraction fit for CMIP5 emissions-forced simulations of RCP 8.5, and (b) Future (2100) vs. contemporary (2010) atmospheric CO_2 mole fraction for the same set of model simulations. The observed atmospheric CO_2 mole fraction is represented by the vertical line at 384.6 ppm with an uncertainty range ($\pm$0.5 ppm) shown in gray. The linear regression model is represented by the blue line surrounded by red dashed lines indicating a 95% confidence interval.*

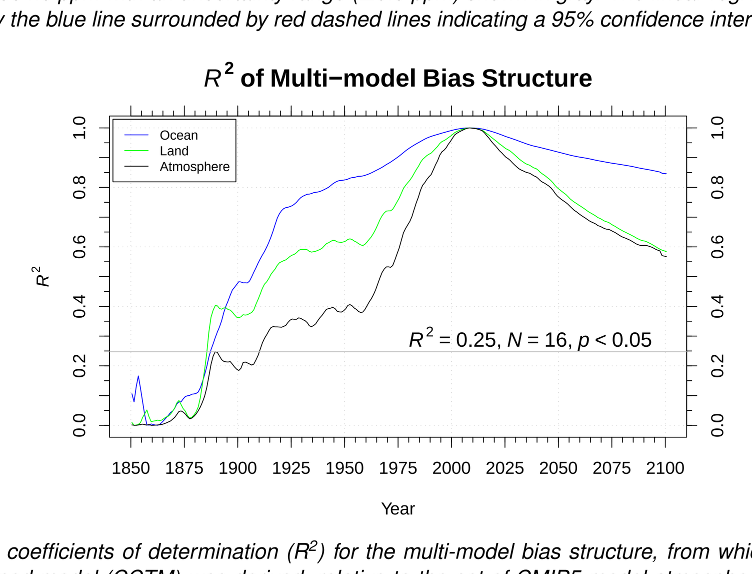

Figure 5: *The coefficients of determination (R^2) for the multi-model bias structure, from which the contemporary CO_2 tuned model (CCTM) was derived, relative to the set of CMIP5 model atmospheric CO_2 (black), ocean (blue), and land (green) predictions in 2010, defined as the 5-y mean for the period 2006–2010.*

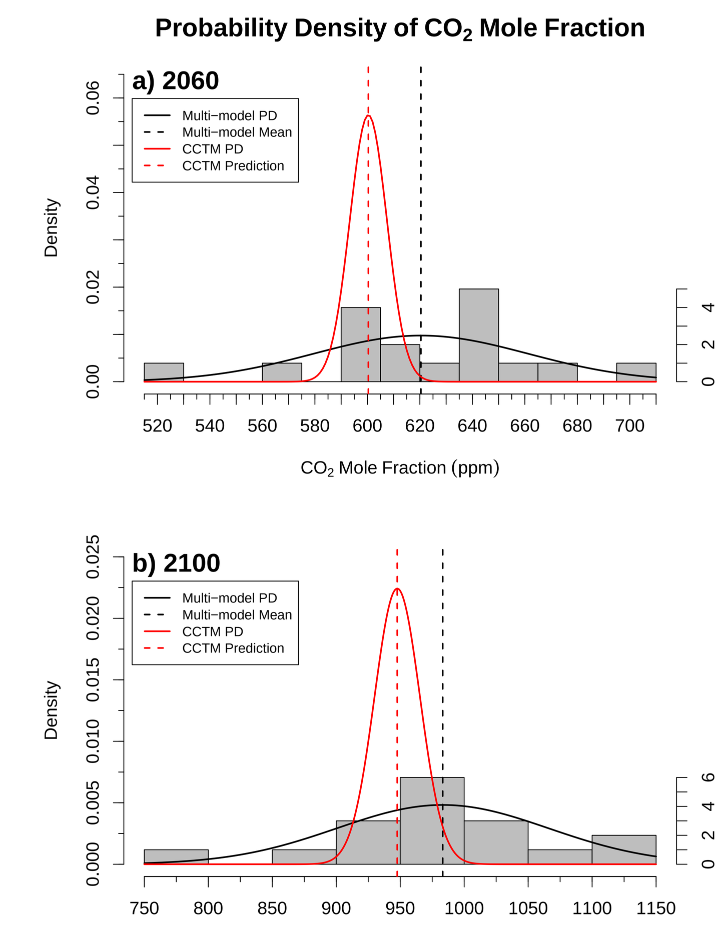

Figure 6: *The probability density of CO_2 mole fraction predictions from the CCTM peaks lower than the probability density for multi-model mean for (a) 2060 and (b) 2100. In addition, the width of the probability density is much smaller for the CCTM, by almost a factor of 6 at 2060 and almost a factor of 5 at 2100, indicating a significant reduction in the range of uncertainty for the CCTM prediction.*

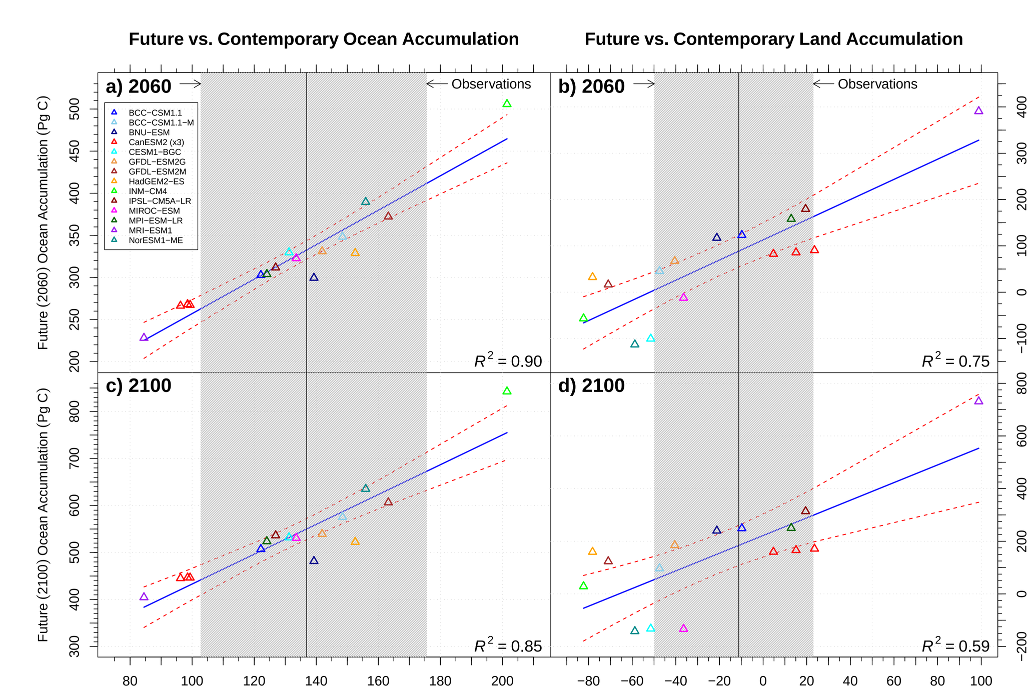

Figure 7: *Future ((a) 2060 and (c) 2100) vs. contemporary (2010) ocean carbon accumulation for CMIP5 emissions-forced simulations of RCP 8.5, and corresponding plots for land carbon accumulation for the same periods ((b) and (d), respectively). Observed contemporary accumulation estimates are shown as vertical lines with an uncertainty range shown in gray. The linear regression model is represented by the blue line surrounded by red dashed lines indicating a 95% confidence interval.*

Implications of a Persistent CO_2 Bias

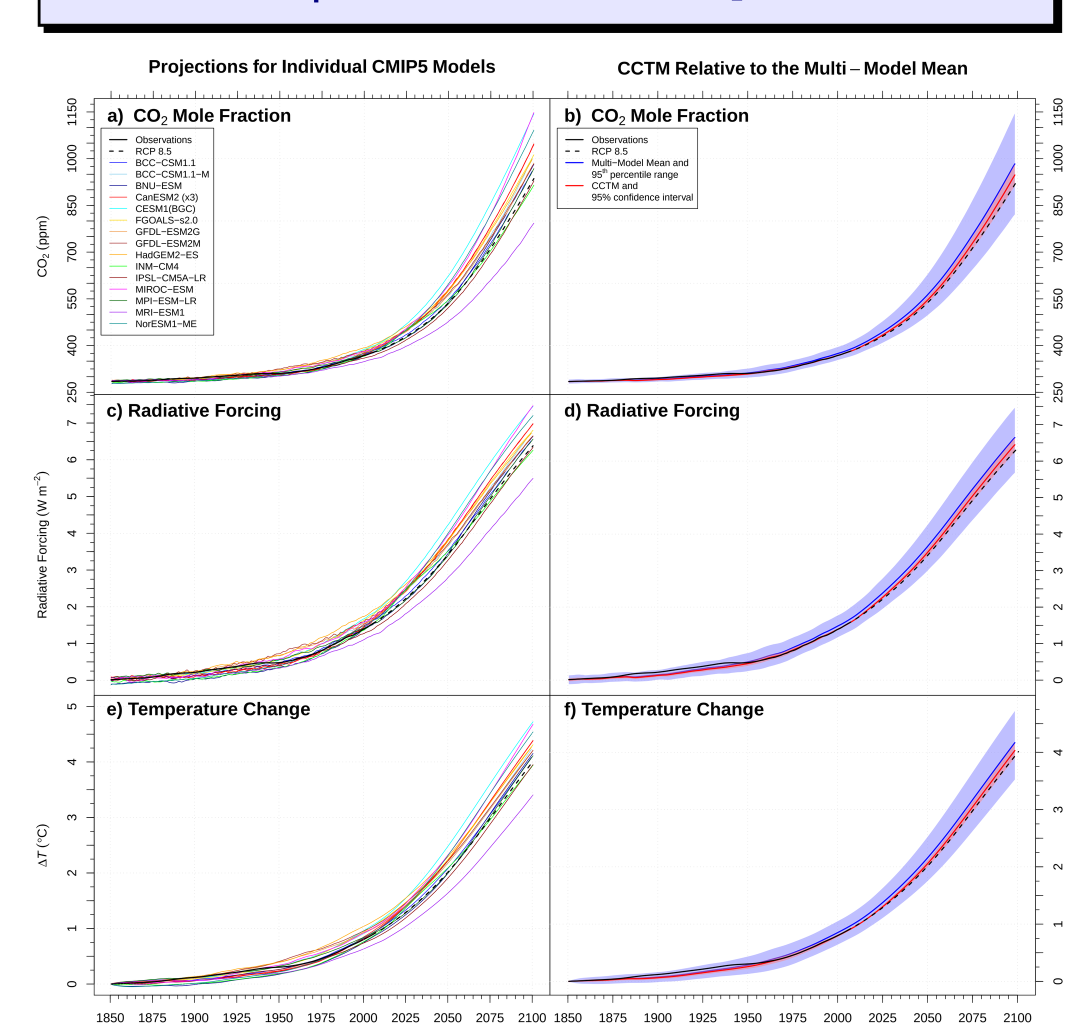

Figure 8: *(a) CO_2 predictions for all CMIP5 models. (b) The contemporary CO_2 tuned model (CCTM) atmospheric CO_2 estimate compared to the CMIP5 multi-model mean trajectory. (c and d) Radiative forcing for all CMIP5 models and the CCTM. (e and f) Temperature changes for all CMIP5 models and the CCTM.*

Discussion and Conclusions

- Many of the processes that contribute to contemporary carbon cycle biases persist over decadal timescales.
- Terrestrial and ocean carbon accumulation compensated for one another within individual models ($R = -0.86$), reducing the bias in predicted atmospheric CO_2.
- The CCTM estimates of atmospheric CO_2 were 21 ppm lower than the multi-model mean in 2060 and 32 ppm lower at 2100, suggesting that stabilization targets may be unnecessarily low.
- Uncertainty estimates derived from this approach were almost 6 times smaller at 2060 and almost 5 times smaller at 2100 than those from the ESM ensemble.
- Community-based model benchmarking (*e.g.*, ILAMB) and model tuning could reduce biases and decrease multi-model spread of future predictions.

See oral presentation on Thursday, 6 June at 14:45, Room 305CD

Acknowledgements

This research was sponsored by the Climate and Environmental Sciences Division (CESD) of the Biological and Environmental Research (BER) Program in the U. S. Department of Energy Office of Science and the National Science Foundation (AGS-1048890). This research used resources of the National Center for Computational Sciences (NCCS) at Oak Ridge National Laboratory (ORNL), which is managed by UT-Battelle, LLC, for the U. S. Department of Energy under Contract No. DE-AC05-00OR22725. CDJ was supported by the Joint DECC/Defra Met Office Hadley Centre Climate Programme (GA01101). The National Center for Atmospheric Research is sponsored by the National Science Foundation. We acknowledge the World Climate Research Programme's Working Group on Coupled Modelling, which is responsible for CMIP, and we thank the climate modeling groups (listed in Table 1 of this poster) for producing and making available their model output. For CMIP the U. S. Department of Energy's Program for Climate Model Diagnosis and Intercomparison provides coordinating support and led development of software infrastructure in partnership with the Global Organization for Earth System Science Portals.